



Application of response surface modelling to economically maximize thorium (IV) adsorption

Nor Azillah Fatimah Othman^{a,b,*}, Sarala Selambakkannu^a, Ting Teo Ming^a, Nor Hasimah Mohamed^a, Takeshi Yamanobe^b, Noriaki Seko^c

^aRadiation Processing Technology, Malaysian Nuclear Agency, Bangi, 43000 Kajang, Malaysia, Tel. +603-8911-2000; emails: azillah@nm.gov.my (N.A.F. Othman), sarala@nm.gov.my (S. Selambakkannu), tmting@nm.gov.my (T.M. Ting), shima@nm.gov.my (N.H. Mohamed)

^bFaculty of Science & Technology, Gunma University, 1-5-1, Tenjin, Kiryu, 376-0052 Gunma, Japan, Tel. +81-277-30-1039; email: yamanobe@gunma-u.ac.jp

^cTakasaki Advanced Radiation Research Institute, Quantum Beam Science Research Directorate, 1233, Watanuki-machi, Takasaki, 370-1292 Gunma, Japan, Tel. +81-27-346-9321; email: seko.noriaki@qst.go.jp

Received 25 April 2019; Accepted 12 October 2019

ABSTRACT

The fibrous adsorbent was synthesized by radiation-induced graft polymerisation with 2-(dimethyl-amino) ethyl methacrylate (DMAEMA). The fibrous grafted substrate with flexible side functional groups was used as an adsorbent to separate Th(IV) ions from an aqueous solution. The properties of the fibrous adsorbents were evaluated by attenuated total reflectance–Fourier-transform infrared spectroscopy, scanning electron microscopy, water uptake capacity and optical contact angle. The effects of adsorbent dosage, initial concentration, and reaction time on the adsorption capacity of the synthesized fibrous adsorbent were optimized using the Box–Behnken design of response surface methodology (RSM). The quadratic model showed an optimal adsorption capacity of 25.13 mg g⁻¹ operating at an initial concentration of 5.5 mg L⁻¹, reaction time of 24 h, and adsorbent dosage of 0.002 g at a maximum desirability value of 1. Under these adsorption conditions, the adsorption capacity of 24.87 mg g⁻¹ was achieved from the experiment indicating good agreement with the predicted value. The applied optimisation procedure of incorporating RSM was effective in achieving the highest adsorption capacity using a minimum adsorbent dosage of only 0.002 g. The results indicate that the use of the fibrous adsorbent is economically promising for the separation of Th(IV) ions.

Keywords: Box–Behnken design (BBD); Response surface methodology (RSM); Thorium; Adsorption; DMAEMA

1. Introduction

Naturally occurring radionuclide materials (NORMs) are radioactive elements present in sand, mineral (ores, igneous and sedimentary rocks) and soil environments. Natural radioactivity in mineral and soil environments include the presence of persistent radionuclides such as uranium (²³⁸U), thorium (²³²Th), potassium (⁴⁰K), radium and its decay product radon (²²⁶Ra) [1]. Industrial activities that exploit

natural resources such as rare earth materials contribute to increased concentrations of radionuclides in wastes. Among the NORMs, thorium (Th) has attracted much attention. This is not only because Th possesses significant radiological impact but also because it is considered a promising alternative nuclear fuel. The study by Wadeah et al. [2] revealed that the average concentration of Th in Malaysian monazite ore is 17,990 ppm.

* Corresponding author.

Similarly, the authors reported that the concentration of Th in the lanthanide concentrate from Lynas Advanced Materials Plant (LAMP) was 1,289 ppm, whereas the water leach purification residue from the plant was 1,952 ppm [3]. In both cases, Th was not recovered as product but was found in the effluent. Therefore, it is crucial to minimize radioactive species such as Th and other radioactive materials using appropriate and effective methods to extract and separate the wastes from a waste management perspective. Solvent extraction is considered the most popular method for the separation of Th [4]. However, solvent extraction has several downsides in terms of selectivity and long extraction time. Furthermore, the numerous hazardous solvents used in the process generate secondary wastes, which pose risks to human health, safety and environment. Therefore, extensive efforts have been made in recent years to solve these problems. Solid extraction is considered a promising and economically viable technique [5] that can be conveniently prepared by radiation grafting. The process of radiation grafting allows the tuning of grafted moieties and the control of the homogeneous grafting yields through various synthesized adsorbents with desired functional groups.

The radiation grafting of 2-(dimethylamino) ethyl methacrylate (DMAEMA) monomer onto polymers has been extensively reported in the literature. Asamoto et al. [6] grafted DMAEMA monomer onto polyethylene (PE) film by photografting. Similarly, the authors co-grafted 2-hydroxyethyl methacrylate (HEMA) and 2-(dimethylamino) ethyl methacrylate (DMAEMA) onto a PE plate by two-step photografting [6]. The product enhanced the effective removal of Cr(VI) ions using (PE-g-PHEMA)-g-PDMAEMA compared with PE-g-DMAEMA [7]. Li et al. [8] prepared Cr(IV) adsorbent by radiation grafting of DMAEMA onto cellulose microsphere (CMS) and grafting of DMAEMA on graphene oxide hybrid materials [9]. Likewise, the DMAEMA was used to synthesize an adsorbent for ionic dye [10,11], phosphate removal [12], adsorption of gold (Au) [13] and other heavy metals such as Cu, Cd, Zn, Pb, Ni [14]. Kavaklı et al. [12] demonstrated the antibacterial activities of grafted PDMAEMA onto a non-woven PE/PP fibre, after quaternization with dimethyl sulfate.

Conversely, the radiation-induced grafting of DMAEMA onto the fibrous non-woven fibre and its utilisation for the removal of Th has not been reported in the literature. There is considerable published literature on the removal of Th using other grafted adsorbents such as hydrogel [15], approximated polyolefin [16,17], nanocomposite [18,19] and graphene [20,21]. However, these studies were conducted through the conventional methods of varying one factor at a time (OFAT), while keeping all other factors constant. The OFAT method of investigating each factor separately is time-consuming. Furthermore, it is incapable of processing multiple variables, particularly if the variables influence the response. Besides, the interactive effects of two or more variables on the system cannot be observed through OFAT, even if several factors dominate the response. Design of experiment (DoE) is a statistical and modelling technique that applies the factorial concept to predict the behaviour of predetermined process variables [22].

Therefore, the response surface methodology (RSM) based Box–Behnken design (BBD) in DoE was employed in

this study to determine the optimum reaction conditions for Th adsorption. The RSM technique resolves the limitations of the OFAT method by reducing the lead time and improving the efficiency of the process. Furthermore, the interaction between the process variables can be explained based on the RSM prediction and the experimental data obtained from the experiment. There are two main types of RSM, namely central composite design (CCD) and BBD. The CCD approach can test extreme conditions of up to five levels per factor, which can fit a full quadratic model. Conversely, the BBD has fewer design points compared with the axial points of the CCD, which is similar to the face-centred composite design ($\alpha = 1$). Therefore, the BBD requires fewer experimental runs for similar numbers of factors, which makes it less expensive and time saving compared with CCD. There are no current researches conducted to optimize the economical use of fibrous grafted adsorbents for the removal of Th from an aqueous solution using the Box–Behnken Design (BBD) method.

Therefore, BBD method of RSM with three (3) levels was employed in this study to optimize the adsorption capacity of the newly prepared fibrous adsorbent in a batch stirred reactor. In due consideration of the economical use of the adsorbent, the adsorbent dosage was set to minimum and the reaction time was extended explicitly beyond the standard practice to ensure complete equilibrium. This will guarantee that the effect of time will have the least influence on the system during the experiments.

2. Methodology

2.1. Synthesis of P-DMAEMA adsorbent

The P-DMAEMA adsorbent was prepared by the radiation-induced grafting method described in our previous work [23,24]. In this study, the 2-(dimethylamino) ethyl methacrylate (DMAEMA) monomer with a mass fraction of 5% was emulsified in ultrapure water in the presence of Tween-20 at 1:0.6 monomer–surfactant ratio using a high-speed homogenizer. The fibrous polyethylene-coated polypropylene-core non-woven fibre (NWF-PE/PP) was irradiated to a total dose of 100 kGy. Next, the emulsion was reacted with irradiated polyethylene-coated polypropylene-core non-woven fibre (NWF-PE/PP) in a water bath for 3 h at 40°C. On completion, the adsorbent was washed with distilled water until the unreacted monomer was eradicated. The adsorbent was subsequently dried in an oven for 24 h and stored in a dry cabinet for further use.

2.2. Adsorption experiments

A total of 17 batch adsorption experiments with a selected range of variables were designed by Box–Behnken Design (BBD) using Design-Expert[®] version 9 (Stat-Ease, Inc, USA). The adsorption experiments for the independent variables were 1–10 mg L⁻¹ for the Th concentration, 0.002–0.005 g for the adsorbent dosage, and 8–24 h for the reaction time. The P-DMAEMA adsorbent with a 100% degree of grafting was used for all experiments. The adsorbent was immersed in 50 mL of solution with an initial pH of 3.5 and stirred under room temperature (25°C) at a predetermined reaction

time (8–24 h). The pH value of 3.5 was selected to prevent precipitation of the Th(IV) ions into hydroxide, which typically occurs at pH values above 4, as explained by Langmuir and Herman [25]. After adsorption, the adsorbent was recovered, and the solution was filtered using a syringe filter (0.45 mm). The concentration of Th in the filtrate was subsequently determined using inductively coupled plasma optical emission spectrometry (ICP-OES). Lastly, the adsorption capacity was determined based on the difference in the Th concentration of the solution, as shown in Eq. (1) [26]:

$$\text{Adsorption capacity} (\text{mg g}^{-1}) = \frac{(C_f - C_i)}{m_{\text{ads}}} \times V_{\text{sol}} \quad (1)$$

where C_i and C_f are the initial and final concentrations (mg L^{-1}), respectively, m_{ads} is the mass of P-DMAEMA, g and V_{sol} is the volume of the solution, L.

2.3. Response surface method of thorium (IV) adsorption by P-DMAEMA

RSM is one of the statistical techniques of DoE that employs regression analysis from collected data to identify the best process performance, interaction effects, and significant factors through optimisation [22,27]. In this study, BBD was employed based on three factors; adsorbent dosage (X_1), initial concentration (X_2), and time (X_3). Therefore, three levels; low (-1), medium (0) and high (+1) of each factor were used to optimize the efficiency of Th(IV) adsorption. The process factors and their levels are presented in Table 1.

Typically, linear or quadratic models are used in the optimisation process of RSM. In this study, the adsorption capacity was optimized based on the selected quadratic model presented in Eq. (2):

$$Y = \alpha_0 + \alpha_1 X_1 + \alpha_2 X_2 + \alpha_3 X_3 + \alpha_{12} X_1 X_2 + \alpha_{13} X_1 X_3 + \alpha_{23} X_2 X_3 + \alpha_{11} X_1^2 + \alpha_{22} X_2^2 + \alpha_{33} X_3^2 \quad (2)$$

where y is the predicted response variable, a_0 is the constant of regression, and the terms a_i , a_{ij} , a_{ij} represent the linear, quadratic, and the interaction coefficients, respectively. The term X_i is the coded variable level, whereas i or j represent the number of independent variables. Each fitted model was examined to ensure that it provides an adequate approximation of the system. The process helps to empirically assess the predictive capabilities of the model and verify that the model satisfies the assumptions of the analysis of variance (ANOVA).

Table 1
Process factors with 3 levels of Box–Behnken

Factors	Designation	Levels of Box–Behnken		
		Low (-1)	Medium (0)	High (+1)
Adsorbent dosage (g)	(X_1)	0.002	0.0035	0.005
Initial concentration (mg L^{-1})	(X_2)	1	5.5	10
Time (h)	(X_3)	8	16	24

2.4. Materials characterisation

In this study, all the chemicals purchased were used without further purification. The NWF-PE/PP fibre was obtained from Kurashiki Textile Manufacturing Co. (Japan). The 2-(dimethylamino) ethyl methacrylate (DMAEMA) was purchased from Tokyo Chemical Industries Co. Ltd. (Japan). The surfactant, Tween-20, was purchased from Kanto Chemical Co. Inc. (Japan).

The Fourier transform infrared (FT-IR) spectra were obtained in the wavenumber region of 4,000–500 cm^{-1} with PerkinElmer Frontier™ spectrometer in attenuated total reflectance (ATR) mode. The morphology and elemental composition/mapping of samples were observed using a scanning electron microscope and energy dispersive X-ray (SEM-EDX Model: Hitachi SU3500/Horiba, Japan) spectroscopy. The surface contact angle was measured with Biolin Attension Theta (Finland) optical contact angle (OCA).

The water uptake test was conducted by immersing DMAEMA grafted NWF-PE/PP in the water at 25°C until equilibrium was reached. The excess water on the surface of the sample was removed using filter paper. The weight of the sample before immersion and after immersion for a predetermined time was weighed. The percentage of water uptake was calculated based on Eq. (3):

$$\text{Water uptake} (\%) = \frac{(W_a - W_b)}{W_b} \times 100 \quad (3)$$

where W_a is the weight of the swelled sample, whereas W_b is the weight of the dry sample.

3. Results and discussion

3.1. Effect of pH

The effect of solution pH is a crucial parameter and plays a vital role in the entire process of adsorption [28]. A consistent increase in adsorption capacity of Th until pH 4 can be seen in Fig. 1a. However, the adsorption capacity decreased beyond pH 4, indicating that the adsorption process is highly affected by pH. At lower pH 1–2, the presence of excessive H^+ ions might interfere and compete with Th ions. Therefore, the process experienced low adsorption of Th. Besides, positively charged surface sites become dominant, which did not favour the positively charged Th cations due to electrostatic repulsion. As the pH increases, a greater number of negatively charged surface sites become available for adsorption to proceed. However, beyond pH 4, the rate

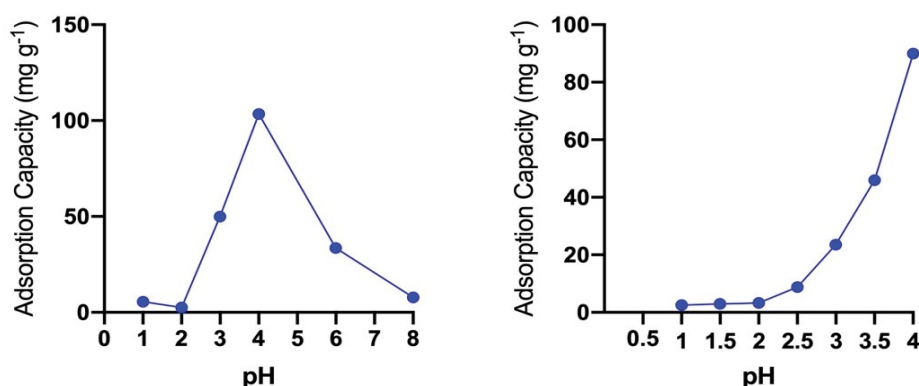


Fig. 1. Effect of pH on adsorption capacity of Th(IV) (adsorption parameter: time = 3 h, initial concentration = 10 ppm, adsorbent dosage = 0.002 g).

of adsorption decreases significantly. This is because hydrolysis of the Th ions negatively affects the adsorption process.

Another adsorption experiment was conducted at pH below 4 at smaller intervals. The same trend, as explained earlier, can be seen from Fig. 1b. The sharp incline from pH 2.5 to 4 indicates that a complex formation between Th(IV) and the active adsorbent sites is promoted. However, Hongxia et al. [29] stated that the precipitation of Th(OH)₄ tends to form at pH > 3.5. Therefore, the sharp increase at pH 4 may be due to this reason. Therefore, pH 3.5 was selected for further investigations.

3.2. Response surface modelling of Thorium(IV) adsorption

The optimisation of the adsorption parameters of Th(IV) on P-DMAEMA was performed to ensure an efficient adsorption capacity over the experimental ranges applied. Hadjittofi and Pashalidis [30] revealed that the highest adsorption capacity in their study was achieved at pH = 3.5 and that $D_s > 100\%$ is sufficient for an adsorbent. However, other parameters influence the adsorption capacity during the adsorption process, such as time, temperature, and adsorbent dosage. The conventional method of simultaneously investigating multiple factors by varying one factor while keeping others constant (OFAT) is time-consuming and prevents analysis of the interactive effects between factors [31].

Therefore, the RSM was employed to determine the optimum process parameters or regions that satisfy the given operational specifications or system. A total of 17 batch adsorption experiments were performed and ANOVA was applied to establish a prediction model for each response. The experimental design, along with the observed data and predicted responses, is presented in Table 2.

The sum of squares and summary statistic tests were conducted to evaluate the adequacy of the models for the adsorption of Th(IV) by P-DMAEMA. The corresponding results are shown in Table 3. The sequential model sum of squares results suggested that the quadratic model provided a good description of the experimental data with “Predicted R^2 ” of 0.9724, indicating good agreement with the “Adjusted R^2 ” of 0.9882.

Furthermore, the high F -value (110.45) and low p -value (<0.0001) indicate that the model is highly significant and the

most appropriate model for further analysis. Therefore, the empirical relationship between the response and the independent variables in the coded units based on the experimental results can be expressed by the quadratic equation:

$$\text{Adsorption capacity}_{\text{Th(IV)}} = 16.29 - 4.80X_1 + 1.97X_2 - 1.15X_3 + 0.14X_1X_2 - 1.51X_1X_3 - 1.50X_2X_3 + 2.70X_1^2 - 3.41X_2^2 + 0.99X_3^2 \quad (4)$$

As presented in Table 4, the ANOVA results for the quadratic model suggests that the model is statistically significant with an F -value of 149.43 and the F -statistical probability value below 0.0001. In this model, X_1 , X_1^2 , X_2 and X_2^2 were highly significant factors, whereas X_3 (time) was significant. All other interactions between the process parameters were significant except for the interaction between the adsorbent dosage and initial concentration (X_1X_2), which was not significant.

The correlation between the observed experimental and the predicted values of adsorption capacity is presented in Fig. 2. The actual values are sensibly distributed near the straight line with $R^2 = 0.99$, indicating a good agreement between the model and experimental data. As observed in Fig. 3, the residuals were distributed mainly in the standard residual plot.

The results for the diagnostic case analysis are presented in Table 5. The value for the predicted and actual response indicates no significant differences, which is evidence of the close correlation between the modelled and measured data. Besides, the leverage value was within the range of 0–1. The internally studentized residual measures the number of standard deviations separating the actual and predicted values.

As observed in Table 5, no lurking or unusual variables were detected in the internally studentized residuals data. The difference in fits or DFFITS is calculated by measuring the influence of the actual value on its predicted value. The DFFITS were found to be between +2 and -2, indicating the absence of any treatments with excessively large influences on the prediction or regression coefficients. Furthermore, Cook’s distance did not detect any outliers, confirming that there is no unusual change in the regression.

Table 2
Experimental design with observed and predicted responses for Th ions adsorption

Run	Factor 1 X_1 : Adsorbent dosage g L ⁻¹	Factor 2 X_2 : Initial concentration mg L ⁻¹	Factor 3 X_3 : Time h	Observed response Adsorption capacity mg g ⁻¹	Predicted response Adsorption capacity mg g ⁻¹
1	0.002	1	16	18.85	18.55
2	0.002	10	16	22.29	22.20
3	0.0035	1	8	11.38	11.55
4	0.0035	5.5	16	15.77	16.29
5	0.002	5.5	24	24.87	25.13
6	0.005	10	16	12.58	12.89
7	0.0035	10	24	13.35	13.18
8	0.0035	5.5	16	16.26	16.29
9	0.0035	10	8	18.54	18.49
10	0.005	1	16	8.58	8.67
11	0.0035	1	24	12.20	12.24
12	0.005	5.5	8	18.11	17.85
13	0.0035	5.5	16	16.72	16.29
14	0.005	5.5	24	12.66	12.52
15	0.0035	5.5	16	15.71	16.29
16	0.002	5.5	8	24.29	24.42
17	0.0035	5.5	16	16.96	16.29

Table 3
Sequential model sum of squares and model summary statistics

Source	Sum of squares	Df	Mean square	F-value	p-value prob. > F	Remarks
Linear	225.69	3	75.23	9.82	0.0012	
2FI	18.19	3	6.06	0.74	0.5496	
Quadratic	79.72	3	26.57	110.45	<0.0001	Suggested
Cubic	0.44	3	0.15	0.47	0.7186	Aliased
Residual	1.24	4	0.31			
Total	4,908.34	17	288.73			
Source	Std. Dev.	Predicted R ²	Adjusted R ²	R ²	Remarks	
Linear	2.77	0.3630	0.6232	0.6938		
2FI	2.85	-0.2694	0.5996	0.7497		
Quadratic	0.49	0.9724	0.9882	0.9948	Suggested	
Cubic	0.56	0.3630	0.9847	0.9962	Aliased	

Therefore, it can be concluded that the analysis of the diagnostic case statistics of the data showed that the model is a good fit for optimising the adsorption capacity for Th.

3.3. Analysis of response surfaces

Using the model acquired, a numerical optimisation procedure for any combination of the four variables, namely adsorbent dosage, initial concentration, time and adsorption capacity of Th can be conducted. The different criteria for the independent variables (adsorbent dosage, initial concentration, time) and dependent variable (adsorption

capacity of Th) can be set accordingly. Therefore, the maximum adsorption capacity was determined using the minimum adsorbent dosage. In this study, the criteria for the procedure was set as “minimum” for adsorbent dosage, “in range” for initial concentration and time, and lastly “maximum” for the adsorption capacity. Fig. 4 exhibits the interactions between the adsorbent dosage (g) with an initial concentration of Th (mg L⁻¹) and time (h) on Th adsorption capacity (mg g⁻¹) that has been optimized with the numerical optimization of RSM. Since the model consists of three factors, Fig. 4 presents the contribution and comparative effects of any possible combination of two independent variables,

Table 4
ANOVA for response surface quadratic model for adsorption of Th(IV)

Source	Sum of squares	df	Mean square	F-value	p-value Prob > F
Model	323.60	9	35.96	149.43	<0.0001
X_1 - Adsorbent dosage	184.04	1	184.04	764.88	<0.0001
X_2 - Initial concentration	30.99	1	30.99	128.81	<0.0001
X_3 - Time	10.65	1	10.65	44.27	0.0003
X_1X_2	0.081	1	0.081	0.33	0.5809
X_1X_3	9.10	1	9.10	37.84	0.0005
X_2X_3	9.00	1	9.00	37.41	0.0005
X_1^2	30.77	1	30.77	127.89	<0.0001
X_2^2	48.98	1	48.98	203.57	<0.0001
X_3^2	4.15	1	4.15	17.24	0.0043
Residual	1.68	7	0.24		
Lack of fit	0.44	3	0.15	0.47	0.7186
Pure error	1.24	4	0.31		
Cor total	325.28	16			
$R^2 = 0.9948$					
$R^2_{\text{adjusted}} = 0.9882$					
$R^2_{\text{predicted}} = 0.9724$					
$A_{\text{req. precision}} = 43.754$					

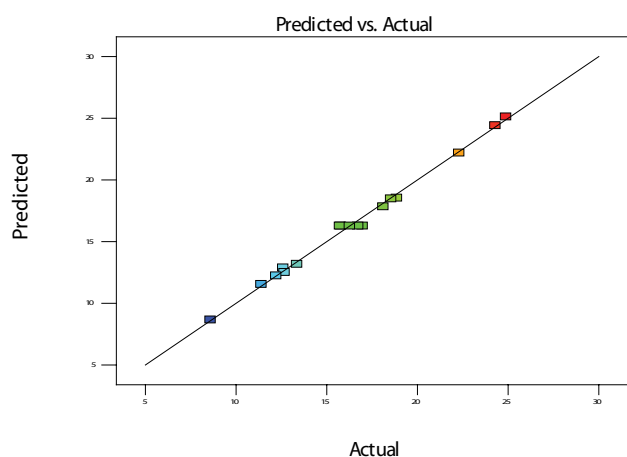


Fig. 2. Relationship between the actual and the predicted value.

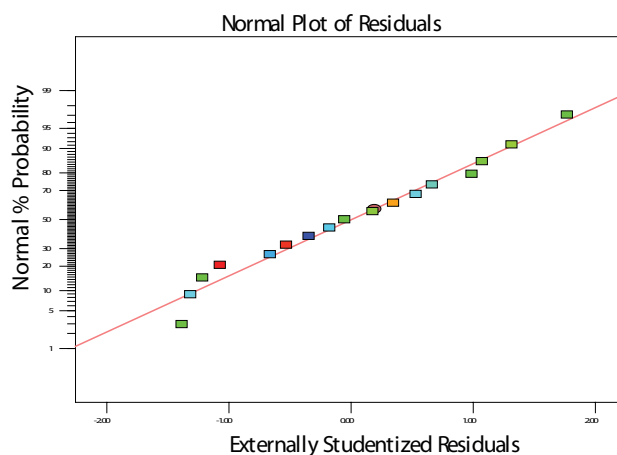


Fig. 3. Plot of studentized residuals.

while keeping another one variable constant. The model predicted an optimal adsorption capacity of 25.13 mg g^{-1} , when the independent variables are 5.5 ppm of the initial concentration and 24 h of reaction time at the maximum desirability value of 1, while the adsorbent dosage was kept constant at 0.002 g .

The graphs suggested that when setting the adsorbent dosage to a minimum, time and initial concentration both have significant effects on the adsorption capacity. It is shown in Figs. 4a and b that the maximum adsorption capacity could be achieved by increasing the reaction time and initial concentration while keeping the adsorbent dosage constant at 0.002 g . In this case, the value of 0.002 g set as the adsorbent

dosage was sufficient. Therefore, the predicted adsorption capacity is in good agreement with the experimental value of 24.87 mg g^{-1} , when the process variables are set according to the optimal values. In Fig. 4a interaction between adsorbent dosage and initial concentration at a constant time of 24 h suggested that an increase in adsorbent dosage at a given initial concentration did not result in higher adsorption capacity. This may be due to the effect of overlapping or screening of the dense outer layer when the number of active sites are beyond optimal [32]. An increase of adsorption capacity with time can be seen in Fig. 4c. However, higher adsorbent dosage is needed to achieve the maximum adsorption capacity at extended time as shown in the figure. This is

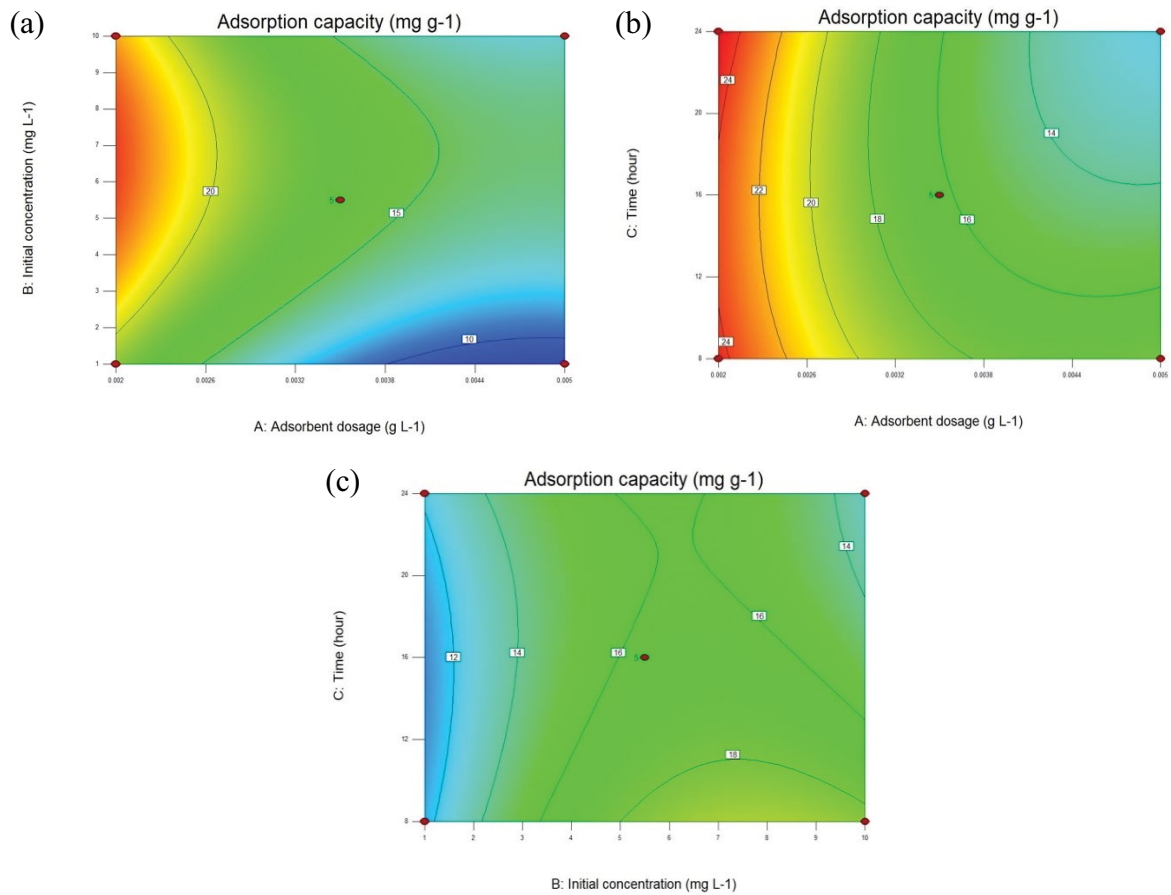


Fig. 4. Effect of interaction between (a) adsorbent dosage and initial concentration, (b) adsorbent dosage and time and (c) initial concentration and time on adsorption capacity.

Table 5
Diagnostic case analysis

Run order	Actual value	Predicted value	Residual	Leverage	Internally studentized residual	Externally studentized residual	Cook's distance	Influence on fitted value DFFITS
1	18.85	18.55	0.31	0.750	1.251	1.315	0.470	2.278
2	22.29	22.20	0.091	0.750	0.370	0.346	0.041	0.599
3	11.38	11.55	-0.17	0.750	-0.691	-0.663	0.143	-1.148
4	15.77	16.29	-0.52	0.200	-1.177	-1.217	0.035	-0.608
5	24.87	25.13	-0.26	0.750	-1.061	-1.073	0.338	-1.858
6	12.58	12.89	-0.31	0.750	-1.251	-1.315	0.470	-2.278
7	13.35	13.18	0.17	0.750	0.691	0.663	0.143	1.148
8	16.26	16.29	-0.026	0.200	-0.059	-0.054	0.000	-0.027
9	18.54	18.49	0.047	0.750	0.190	0.177	0.011	0.306
10	8.58	8.67	-0.091	0.750	-0.370	-0.346	0.041	-0.599
11	12.20	12.24	-0.047	0.750	-0.190	-0.177	0.011	-0.306
12	18.11	17.85	0.26	0.750	1.061	1.073	0.338	1.858
13	16.72	16.29	0.43	0.200	0.990	0.988	0.024	0.494
14	12.66	12.52	0.14	0.750	0.560	0.531	0.094	0.919
15	15.71	16.29	-0.57	0.200	-1.303	-1.386	0.042	-0.693
16	24.29	24.42	-0.14	0.750	-0.560	-0.531	0.094	-0.919
17	16.96	16.29	0.68	0.200	1.549	1.769	0.060	0.884

due to the need of a larger number of surface sites to accommodate the larger number of Th ions. On the other hand, the interaction between the initial concentration and time at a constant adsorbent dosage of 0.002 g was considered less significant, based on Fig. 4c. It was suggested that increase or decrease beyond the optimum level of time and initial concentration at a constant adsorbent dosage did not result in higher adsorption capacity. This supports the earlier observation of interaction between adsorbent dosage and time.

Keshtkar and Mousavian [33] used CCD RSM to optimize the process parameters for Th(IV) removal using a commercial product, Amberlite IR-120 and IRA-400. The adsorption capacities of Th(IV) onto IR-120, IRA-400, and IR-120 + IRA-400 under optimized conditions were 24.15, 2.43 and 13.11 mg g⁻¹, respectively. Therefore, it can be concluded that P-DMAEMA used in this study is comparable with commercially available resins.

As mentioned previously, radiation-induced grafting of DMAEMA onto fibrous non-woven fibre for removal of Th has not been previously reported in the literature. However, DMAEMA is a common monomer used for the preparation of grafted adsorbent for heavy and toxic metals [34–36]. Previous research works on DMAEMA-grafted adsorbent showed that high adsorption capacity could be observed for a metal ion with a smaller ionic radius, as presented in Table 6. Many researchers have explained the sequence of the adsorption process, which typically starts from the hydrolysis reaction of metal ions in aqueous solutions. The adsorption of the metal ions on the adsorbent will follow right after the hydrolysis. More significant ions are hydrolysed compared with smaller ions; and therefore, have lower adsorption capacities compared with the smaller ions.

The findings of Igwe and Abia [41] support the observation that adsorption capacity increases with decreasing ionic radii as follows: Zn²⁺(0.74 Å) > Cd²⁺(0.97 Å) > Pb²⁺(1.20 Å). As observed, the adsorption capacity of the adsorbent prepared in this study for Th ions is comparable with data in the literature. However, the rate of adsorption varies in terms of the selected experimental conditions. Therefore, it is difficult to directly compare the synthesized adsorbent in this study to others reported in the literature.

3.4. Material characterizations

The attenuated total reflectance–Fourier-transform infrared spectroscopy spectrum of the ungrafted NWF-PE/PP

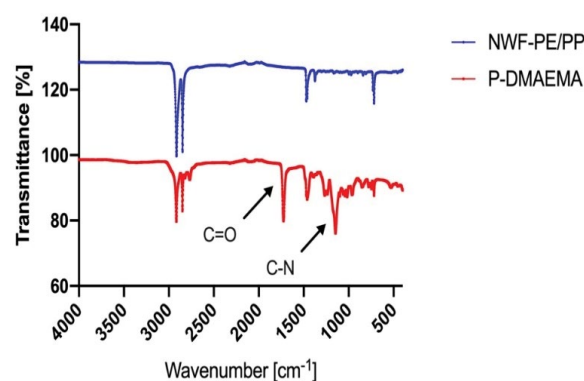


Fig. 5. FT-IR spectra of pristine NWF-PE/PP (blue) and P-DMAEMA (red).

sample is shown in Fig. 5. The characteristic peaks for pristine PE/PP were observed at 2,916 and 2,848 cm⁻¹ corresponding to –CH₂ stretching vibrations. The new vibration bands observed at 1,724 and 1,146 cm⁻¹ are characteristic of –C=O and –C–N of DMAEMA, implying the successful grafting of DMAEMA onto the NWF-PE/PP.

The water uptake test and OCA test were performed to observe the surface wettability of the samples. Fig. 6a shows equilibrium water uptake of P-DMAEMA and Fig. 6b shows the OCA image for P-DMAEMA. The significant increase in water uptake with time can be observed in the figure. However, this value became stagnant after 2 h, indicating that the P-DMAEMA water-absorbing capacity had reached its saturation point. The contact angle for the P-DMAEMA was observed from 113° to 118°, implying that the polymer is slightly hydrophobic after RIGP due to comparatively less hydrophilic nature of the DMAEMA monomer. However, this value is still acceptable for adsorption based on the water uptake test results discussed earlier.

Fig. 7a shows the SEM image of DMAEMA grafted NWF-PE/PP (P-DMAEMA), while Fig. 7b shows the SEM image of the P-DMAEMA containing Th. The heterogeneity and surface roughness were transformed, resulting from the adsorption of Th on the fibrous adsorbent. The EDX image showed the distribution of Th across the surface of the fibrous adsorbent in Fig. 7c. The results confirm the adsorption and distribution of Th onto the surface of the prepared fibrous adsorbent.

Table 6
Comparative adsorption capacities of different DMAEMA grafted adsorbents

Precursors/support	Target elements	Ionic radii (Å)	Initial concentration	Q/pH	Ref.
PP films	Phosphate, PO ₄ ³⁻	2.38 ^a	25 ppm	2.85 mg g ⁻¹ at pH 7.2	[37]
PP films	Nitrate, NO ₃ ⁻	1.79 ^a	25 ppm	3.4 mg g ⁻¹ at pH 7.2	[37]
PE/PP nonwoven fabric	Thorium, Th ⁴⁺	1.08	5.5 ppm	24.87 mg g ⁻¹ at pH 3.5	The present study
PE/PP nonwoven fibres	Arsenic, As ⁵⁺	0.60	10 ppm	83.33 mg g ⁻¹ at pH 7	[38]
Silica	Arsenic, As ⁵⁺	0.60	100 ppm	44.3 mg g ⁻¹ at pH 7	[39]
Cellulose microsphere (CMS)	Chromium Cr ⁶⁺	0.58	100 ppm	78.8 mg g ⁻¹ at pH 4	[40]
Silica	Chromium Cr ⁶⁺	0.58	100 ppm	51.9 mg g ⁻¹ at pH 5	[39]

^aThermochemical radii.

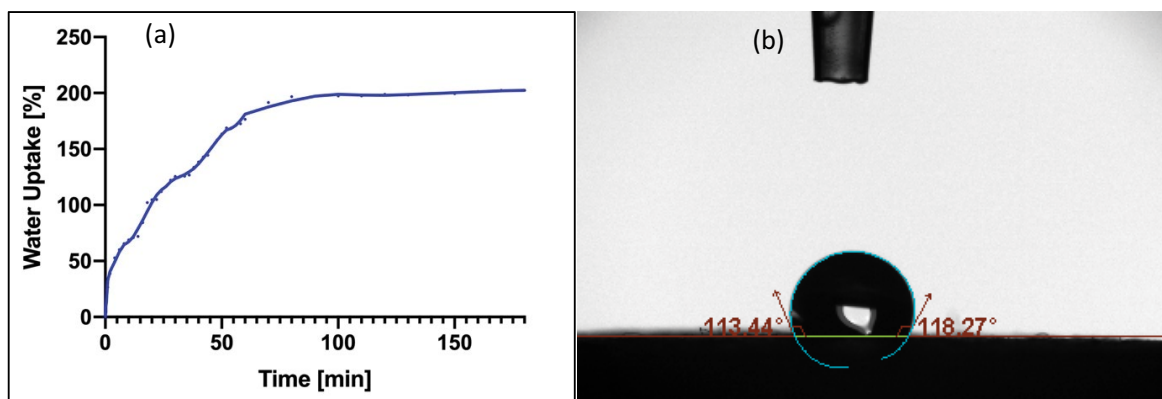


Fig. 6. (a) Water uptake of P-DMAEMA at 25°C, and (b) contact angle image of P-DMAEMA.

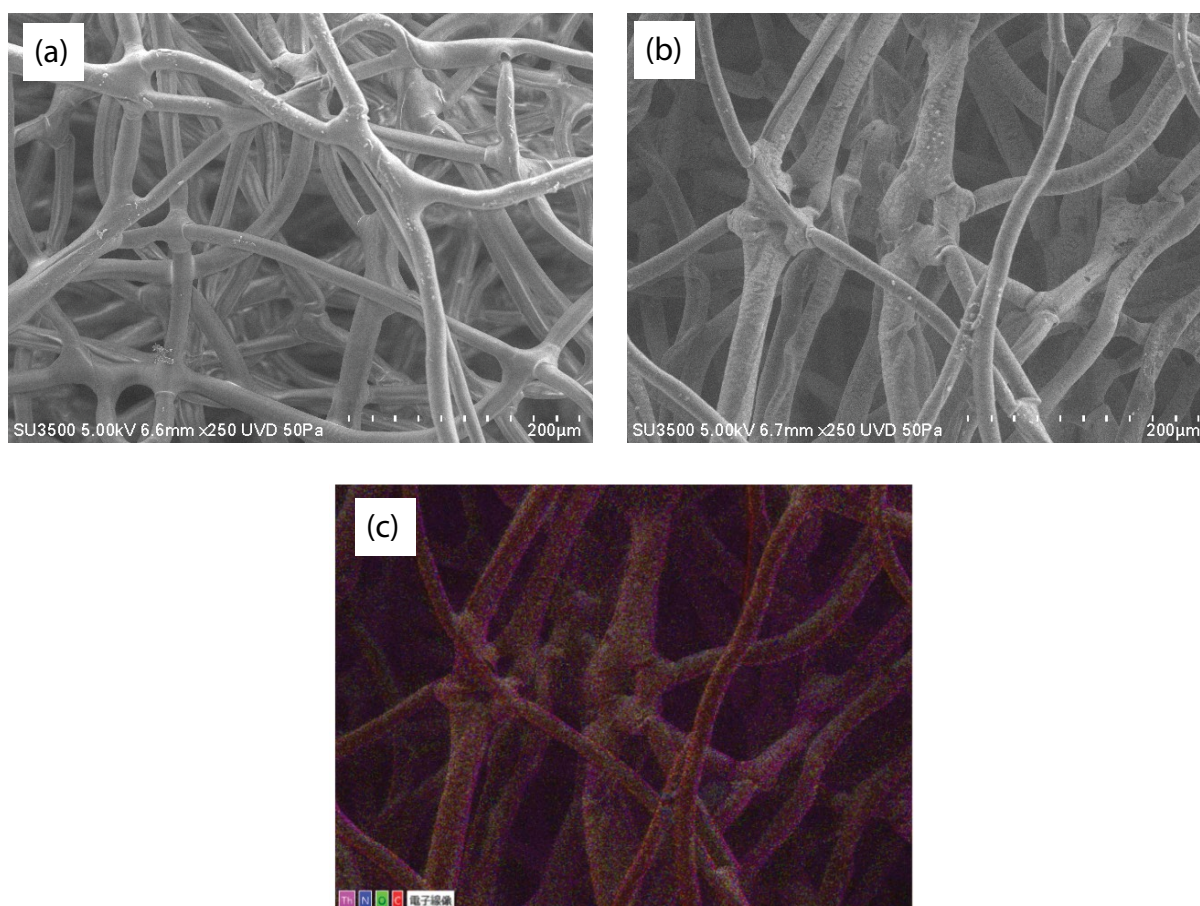


Fig. 7. (a) SEM image of P-DMAEMA (percentage of grafting = 100%), (b) SEM image of P-DMAEMA containing Th, and (c) EDX mapping of P-DMAEMA after Th adsorption. (adsorption conditions: initial concentration 5.5 ppm, pH 3.5, and 24 h adsorption time).

4. Conclusion

The present study revealed that the newly prepared fibrous radiation grafted adsorbent was effective in the removal of Th(IV) from an aqueous solution. The uptake capacity and economical usage of the adsorbent were optimized using Box–Behnken design by adapting the desirability function. The optimal adsorption capacity of 25.13 mg g⁻¹ was predicted at an initial concentration of 5.5 mg L⁻¹,

the reaction time of 24 h, and adsorbent dosage of 0.002 g. This predicted adsorption capacity was in good agreement with the experimental value of 24.87 mg g⁻¹.

Acknowledgements

Financial support was provided by the Ministry of Environment, Science, Technology and Climate Change

(MESTECC), Malaysia (FP0214D052 DSTIN) and Japan Society for Promoting Science (JSPS), Japan, under the RONPAKU program (R11703) awarded to N.A.F. Othman. The authors declare no conflict of interest.

References

- [1] N. Ahmad, M.S. Jaafar, M. Bakhsh, M. Rahim, An overview on measurements of natural radioactivity in Malaysia, *J. Rad. Res. Appl. Sci.*, 8 (2015) 136–141.
- [2] M. Wadeah, N.A.C.Z.B. Che, A.M. Amran, S. Sukiman, Separation and radiological impact assessment of thorium in Malaysian monazite processing, *Malaysian J. Anal. Sci.*, 20 (2016) 770–776.
- [3] W.M. Al-Areqi, A.A. Majid, S. Sarmani, Thorium, Uranium and Rare Earth Elements Content in Lanthanide Concentrate (LC) and Water Leach Purification (WLP) Residue of Lynas Advanced Materials Plant (LAMP), in: AIP Conference Proceedings, AIP, 2014, pp. 93–96.
- [4] Y. Lu, H. Wei, Z. Zhang, Y. Li, G. Wu, W. Liao, Selective extraction and separation of thorium from rare earths by a phosphorodiamidate extractant, *Hydrometallurgy*, 163 (2016) 192–197.
- [5] Y. Sun, A.G. Chmielewski, Applications of Ionizing Radiation in Materials Processing, Institute of Nuclear Chemistry and Technology, 2017.
- [6] H. Asamoto, Y. Kimura, Y. Ishiguro, H. Minamisawa, K. Yamada, Use of polyethylene films photografted with 2-(dimethylamino) ethyl methacrylate as a potential adsorbent for removal of chromium (VI) from aqueous medium, *J. Appl. Polym. Sci.*, 133 (2016) 43360.
- [7] K. Yamada, Y. Ishiguro, Y. Kimura, H. Asamoto, H. Minamisawa, Two-step grafting of 2-hydroxyethyl methacrylate (HEMA) and 2-(dimethylamino) ethyl methacrylate (DMAEMA) onto a polyethylene plate for enhancement of Cr (VI) ion adsorption, *Environ. Technol.*, 40 (2019) 855–869.
- [8] C. Li, Y. Zhang, J. Peng, H. Wu, J. Li, M. Zhai, Adsorption of Cr(VI) using cellulose microsphere-based adsorbent prepared by radiation-induced grafting, *Rad. Phys. Chem.*, 81 (2012) 967–970.
- [9] H.-L. Ma, Y. Zhang, L. Zhang, L. Wang, C. Sun, P. Liu, L. He, X. Zeng, M. Zhai, Radiation-induced graft copolymerization of dimethylaminoethyl methacrylate onto graphene oxide for Cr(VI) removal, *Rad. Phys. Chem.*, 124 (2016) 159–163.
- [10] J. Karthika, B. Vishalakshi, Novel stimuli responsive gellan gum-graft-poly (DMAEMA) hydrogel as adsorbent for anionic dye, *Int. J. Biol. Macromol.*, 81 (2015) 648–655.
- [11] P.B. Krishnappa, V. Badalamoole, Karaya gum-graft-poly (2-(dimethylamino) ethyl methacrylate) gel: An efficient adsorbent for removal of ionic dyes from water, *Int. J. Biol. Macromol.*, 122 (2019) 997–1007.
- [12] P.A. Kavaklı, C. Kavaklı, N. Seko, M. Tamada, O. Güven, Radiation-induced grafting of dimethylaminoethylmethacrylate onto PE/PP nonwoven fabric, *Nucl. Instrum. Methods Phys. Res. Sect. B*, 265 (2007) 204–207.
- [13] X. Liu, J. Ao, X. Yang, C. Ling, B. Zhang, Z. Wang, M. Yu, R. Shen, H. Ma, J. Li, Green and efficient synthesis of an adsorbent fiber by preirradiation-induced grafting of PDMAEMA and its Au (III) adsorption and reduction performance, *J. Appl. Polym. Sci.*, 134 (2017) 44955.
- [14] Y. Bai, Y.N. Liang, X. Hu, An eco-friendly approach for heavy metal adsorbent regeneration using CO₂-responsive molecular octopus, *Chemosphere*, 185 (2017) 1157–1163.
- [15] G. Duan, Q. Zhong, L. Bi, L. Yang, T. Liu, X. Shi, W. Wu, The poly (acrylonitrile-co-acrylic acid)-graft- β -cyclodextrin hydrogel for thorium (IV) adsorption, *Polymers*, 9 (2017) 201.
- [16] J. Xiong, S. Hu, Y. Liu, J. Yu, H. Yu, L. Xie, J. Wen, X. Wang, Polypropylene modified with amidoxime/carboxyl groups in separating uranium (VI) from thorium (IV) in aqueous solutions, *ACS Sustain. Chem. Eng.*, 5 (2017) 1924–1930.
- [17] C. Jin, J. Hu, J. Wang, C. Xie, Y. Tong, L. Zhang, J. Zhou, X. Guo, G. Wu, An amidoximated-UHMEPE fiber for selective and high efficient removal of uranyl and thorium from acid aqueous solution, *Adv. Chem. Eng. Sci.* 7 (2017) 45–59.
- [18] A. Mittal, R. Ahmad, I. Hasan, Poly (methyl methacrylate)-grafted alginate/Fe₃O₄ nanocomposite: synthesis and its application for the removal of heavy metal ions, *Desal. Wat. Treat.*, 57 (2016) 19820–19833.
- [19] F.E. Soetaredjo, S. Ismadji, K. Foe, J. Yi-Hsu, Recent Advances in the Application of Polymer-Based Nanocomposites for Removal of Hazardous Substances from Water and Wastewater, in: *New Polymer Nanocomposites for Environmental Remediation*, Elsevier, 2018, pp. 499–540.
- [20] M. Chen, Z. Li, Y. Geng, H. Zhao, S. He, Q. Li, L. Zhang, Adsorption behavior of thorium on N, N, N', N'-tetraoctyldiglycolamide (TODGA) impregnated graphene aerogel, *Talanta*, 181 (2018) 311–317.
- [21] M. Gado, Sorption of thorium using magnetic graphene oxide polypyrrole composite synthesized from water hyacinth roots, *Iran. J. Chem. Chem. Eng. Res.*, 37 (2018) 145–160.
- [22] M.J. Anderson, P.J. Whitcomb, RSM Simplified: Optimizing Processes Using Response Surface Methods for Design of Experiments, Productivity Press, 2016.
- [23] S. Selambakkannu, N.A.F. Othman, K.A. Bakar, Z.A. Karim, Adsorption studies of packed bed column for the removal of dyes using amine functionalized radiation induced grafted fiber, *SN Appl. Sci.*, 1 (2019) 175.
- [24] N. Othman, S. Selambakkannu, T. Ting, A. Zulkhairun, Modification of kenaf fibers by single step radiation functionalization of 2-hydroxyl methacrylate phosphoric acid (2-HMPA), *SN Appl. Sci.*, 1 (2019) 220.
- [25] D. Langmuir, J.S. Herman, The mobility of thorium in natural waters at low temperatures, *Geochim. Cosmochim. Acta*, 44 (1980) 1753–1766.
- [26] J.K. Singh, N. Verma, Aqueous Phase Adsorption: Theory, Simulations and Experiments, CRC Press, 2018.
- [27] A. Kumar, B. Prasad, I. Mishra, Optimization of process parameters for acrylonitrile removal by a low-cost adsorbent using Box–Behnken design, *J. Hazard. Mater.*, 150 (2008) 174–182.
- [28] Z. Wei, K. Liang, Y. Wu, Y. Zou, J. Zuo, D.C. Arriagada, Z. Pan, G. Hu, The effect of pH on the adsorption of arsenic (III) and arsenic (V) at the TiO₂ anatase [1 0 1] surface, *J. Colloid Interface Sci.*, 462 (2016) 252–259.
- [29] Z. Hongxia, W. Xiaoyun, L. Honghong, T. Tianshe, W. Wangsuo, Adsorption behavior of Th (IV) onto illite: effect of contact time, pH value, ionic strength, humic acid and temperature, *Appl. Clay Sci.*, 127 (2016) 35–43.
- [30] L. Hadjittofi, I. Pashalidis, Thorium removal from acidic aqueous solutions by activated biochar derived from cactus fibers, *Desal. Wat. Treat.*, 57 (2016) 27864–27868.
- [31] R.H. Myers, D.C. Montgomery, C. Anderson-Cook, Process and product optimization using designed experiments, *Response surface methodology*, 4 (2002) 328–335.
- [32] A. Dąbrowski, Adsorption—from theory to practice, *Adv. Colloid Interface Sci.*, 93 (2001) 135–224.
- [33] A.R. Keshtkar, M.A. Mousavian, Application of response surface methodology for thorium (IV) removal using Amberlite IR-120 and IRA-400: ion exchange equilibrium and kinetics, *J. Part. Sci. Technol.*, 3 (2017) 101–112.
- [34] Z. Kong, X. Wu, J. Wei, H. Zhang, L. Cui, Preparation and characterization of hydrophilicity fibers based on 2-(dimethylamino) ethyl methacrylate grafted polypropylene by UV-irradiation for removal of Cr (VI) and as (V), *J. Polym. Res.*, 23 (2016) 199.
- [35] J.F. Madrid, M. Barsbay, L. Abad, O. Güven, Grafting of N, N-dimethylaminoethyl methacrylate from PE/PP nonwoven fabric via radiation-induced RAFT polymerization and quaternization of the grafts, *Rad. Phys. Chem.*, 124 (2016) 145–154.
- [36] K. Saito, K. Fujiwara, T. Sugo, Revolution in the Form of Polymeric Adsorbents 2: Fibers, Films, and Particles, in: *Innovative Polymeric Adsorbents*, Springer, 2018, pp. 109–143.
- [37] M.F.A. Taleb, G.A. Mahmoud, S.M. Elsigeny, E.-S.A. Hegazy, Adsorption and desorption of phosphate and nitrate ions

- using quaternary (polypropylene-gN, N-dimethylamino ethyl-methacrylate) graft copolymer, *J. Hazard. Mater.*, 159 (2008) 372–379.
- [38] C. Kavaklı, P.A. Kavaklı, B.D. Turan, A. Hamurcu, O. Güven, Quaternized dimethylaminoethyl methacrylate strong base anion exchange fibers for As (V) adsorption, *Rad. Phys. Chem.*, 102 (2014) 84–95.
- [39] L. Zhao, J. Sun, Y. Zhao, L. Xu, M. Zhai, Removal of hazardous metal ions from wastewater by radiation synthesized silica-graft-dimethylaminoethyl methacrylate adsorbent, *Chem. Eng. J.*, 170 (2011) 162–169.
- [40] C. Li, Y. Zhang, J. Peng, H. Wu, J. Li, M. Zhai, Adsorption of Cr (VI) using cellulose microsphere-based adsorbent prepared by radiation-induced grafting, *Rad. Phys. Chem.*, 81 (2012) 967–970.
- [41] J.C. Igwe, A.A. Abia, Adsorption isotherm studies of Cd (II), Pb (II) and Zn (II) ions bioremediation from aqueous solution using unmodified and EDTA-modified maize cob, *Eclética Química*, 32 (2007) 33–42.